# Magnetic catalyst residues and their influence on the field electron emission characteristics of low temperature grown carbon nanotubes

Yun-Hi Lee[a)]
*National Research Laboratory, Department of Physics, Korea University, Seoul 136-713, Korea and Nano Devices and Physics Laboratory, Department of Physics, Korea University, Seoul 136-713, Korea*

D. H. Kim
*Yeungnam University, Kyungsan 712-749, Korea*

Dong Hyun Kim
*Department of Chemical Engineering, Kyungpook National University, Daegu 702-701, Korea*

Byeong-Kwon Ju
*College of Engineering, Korea University, Seoul 136-701, Korea*

(Received 3 December 2005; accepted 29 June 2006; published online 24 August 2006)

We report the electron paramagnetic resonance characteristics of catalytic residues for *in situ* grown carbon nanotube field electron emitter and present direct evidence that field electron emission in carbon nanotube sheets grown on various catalytic nanodots/$SiO_2$-coated Si substrate with low-pressure chemical vapor deposition is influenced by the magnetism of catalytic metals and thus the electrical properties of the nanotubes. The nanotubes with weak trace of ferromagnetism, which originated from the catalysts, show lower turn-on emission field and higher electron emission current than those with distinct ferromagnetic properties. A strong relationship between the ferromagnetism of nanocrystalline catalysts and field electron emission characteristics of nanotubes can be utilized for the development of an efficient carbon nanotube based-field electron emitter. © *2006 American Institute of Physics*. [DOI: 10.1063/1.2267342]

One of the interesting applications of carbon nanotubes (CNTs) is field electron emission, and in this case, the direct growth of CNTs on a predefined structure is an ideal process that does not require additional posttreatment. Nanotube production involves the widespread use of transition metal (TM) catalysts such as Ni, Co, or Fe, and field emission experiments have shown that CNTs, regardless of whether they are diode or triode type, are excellent field electron emitters with high current density under a relative low electric field.[1–10] The emission behavior has been related to the localized electronic states at the nanotube tips, space-charge effects, and other adsorbates. Here, note that in most cases, one cannot rule out the effect of the existence of catalytic metals on the tip ends of CNTs or in outer sites such as bridge and atop sites on the C–C bonds.[11–14]

On the other hand, Binh[15] *et al.* studied a splitting of the electron beams for the nanotips as an atomic scale beam splitter. This phenomenon was explained as the strong magnetic interaction at the apex of the nanosized ferromagnetic electron emitter.

Shen *et al.* reported the systematic results of electron spin resonance (ESR) [or electron paramagnetic resonance (EPR)] study on the electronic structures of CNTs provided by different manufacturers and synthesized by a variety of methods before and after purification of catalytic metal.[16]

Through the above mentioned works on CNTs the existence of the interaction of TM atoms on or inside the carbon nanotubes offers another related and challenging problem. *In this work*, we prepared CNTs on thermally grown $SiO_2$-coated Si wafer substrate with the magnetron sputtered catalytic nickel metals by chemical vapor deposition. Here, we present new results of electron spin resonance measurements as well as field emission properties for the as-grown CNTs without any purification processes. Based on the obtained results, we discuss the effect of the existence of magnetism of catalytic metal on the electron emission properties of CNTs. This is the first observation of the catalytic metal effects on the emission behavior of *in situ* vertically grown CNTs.

Catalytic Ni nanodots were grown on a thermally grown $SiO_2$-coated Si substrate by radio frequency magnetron sputtering method. Ferromagnetic resonance spectra to examine magnetic properties of the catalyst were recorded by a Bruker ESP-300S spectrometer operating at 9.8 GHZ equipped with a variable temperature accessory. Field electron emission properties of the CNT the cathode electrodes under the vacuum pressure of about $10^{-7}$ torr.

SEM images can give more direct information on the microscopic structure and uniformity of the Ni film surface. Plane-view images of the annealed Ni films is illustrated in Fig. 1. As shown in the figure, the most frequent grain size is about 100 nm and the separation distance between nanodots is nearly about 10–300 nm. The formation of single or multiple catalytic nanodots on a $SiO_2$-coated Si substrate is understood by now.[17] As-deposited Ni films have an intrinsic tensile stress of $\sim 8\times 10^9$ dyn/cm$^2$. However, upon heating, these films develop compressive stress due to the different thermal expansion coefficients of Ni ($13\times 10^{-6}/°C$) and $SiO_2$ ($5\times 10^{-7}/°C$). At 650 °C, the net stress will be compressive. Furthermore, the compressively strained Ni film will develop propagating sinusoidal wrinkles to minimize the strain energy. This will tend to break thin films into small patches, and at elevated temperatures, metastable Ni patches will tend to form clusters to further reduce the strain energy. Large size dots break into multiple smaller dots, whereas

[a)]Author to whom correspondence should be addressed; electronic mail: yhlee@korea.ac.kr

 

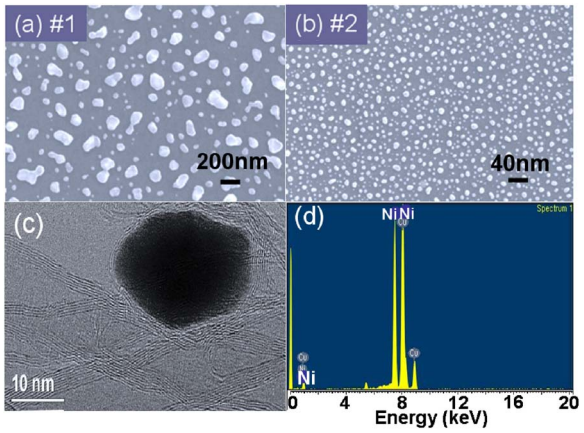


FIG. 1. (Color online) Typical SEM photographs of the catalytic nanodots of (a) 10-nm-thick Ni and (b) 5-nm thick Ni before the growth of CNTs. The size of nanodots varies with the change of the thickness of the catalytic metal. (c) An enlarged HRTEM image showing the existence of residue at tip end of CNT. (d) The residue is identified as Ni through energy dispersive spectra of the tip end (c).

smaller dots below a critical size form only a single nanodot. Finally, the breakup does not occur because the increase of the surface energy becomes larger than the reduction of the strain energy. Figure 1(c) shows an image of CNTs observed by high resolution transmission electron microscopic (HR-TEM) measurement, showing three- or five-walled carbon nanotubes with a larger catalytic residue, which was identified clearly as Ni, as shown in Fig. 1(d).

The angle dependent ferromagnetic resonance (FMR) spectra at room temperature were obtained for the catalytic layer after formation of nanodots. These spectra are useful for examining the mechanical stress induced in ferromagnetic thin films because the resonance field depends sensitively on the stress induced by magnetostriction during nanodot formation. A typical single and wide FMR peak was observed in Ni nanodots, as shown in Fig. 2(a), and the dependence of the resonance field on the angle of the applied magnetic field was clearly shown. The approximate $g$ value of 2.5 well agreed with the $g$ factors for metallic Ni. The resonance linewidth $\Delta H$, which originates essentially from internal field inhomogeneity, and the spatial variations of Ni

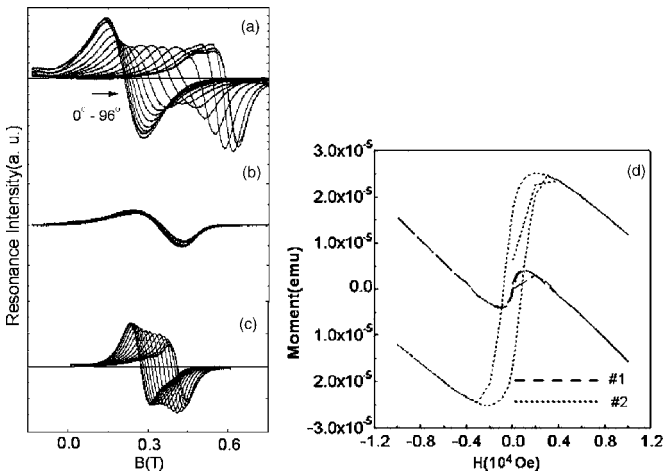


FIG. 2. (a) Ferromagnetic resonance spectra for the catalytic nanodots of Ni just before the growth of CNTs. (b) CNTs with (a) of Fig. 1 and (c) CNTs with (b) of Fig. 1. (d) Typical magnetization-applied field loops for the Ni nanodot corresponding to (b) and (c).

of different crystallites were measured with the applied magnetic field parallel and perpendicular to the specimen. The $\Delta H_{\perp}$ for the nanodots is slightly larger than $\Delta H_{\parallel}$. Usually, highly anisotropic polycrystalline samples are characterized by large $\Delta H$ values, around 0.1–0.15 T. This is due mainly to their large magnetocrystalline and shape anisotropies. Because of random orientations of nanocrystallites and demagnetization fields, different crystallites resonate at different fields, broadening the resonance line in the specimens. The decrease of the linewidths with increasing temperature is very similar to the variation in the way that resonance field increases with temperature, implying that the anisotropy factor may determine the linewidth $\Delta H$.

Next, we examine the spectra for the CNT layer onto the nanodots. The spectra showed a clear trace of the ferromagnetic nanodots, as illustrated in Figs. 2(a)–2(c), suggesting both the existence of crystalline catalyst even after the CNT growth and the strong anisotropic properties of CNTs. The resonance spectra for the CNT specimens showed dramatic changes with the annealing condition of Ni catalytic metal. The difference between 1 (10-nm-thick Ni, $T_{\mathrm{CNT}} \sim 650\ ^{\circ}\mathrm{C}$) and 2 (5-nm-thick Ni, $T_{\mathrm{CNT}} \sim 650\ ^{\circ}\mathrm{C}$) is the thickness of the catalytic metal Ni for the growth of CNTs. The angle dependence of the resonance spectra is in the order of $3 > 2 > 1$. Compared with the spectra for the Ni nanodots before the growth of the CNT [Fig. 2(a)], we observed an increase in signal intensity of FMR due to catalytic metal (CM) with the decrease of the thickness of CMs. While resonance field shifted toward the same direction with the growth temperature, signal intensity due to magnetic catalysts increased. Although the resonance peak, which consisted of a broad FMR from Ni and a narrow line from conduction electron spin resonance[16,17] from multiwalled nanotube, was observed in all specimens, the FMR intensity was changed with the thickness of CM. The strong dependence of signal intensity on the angle is related to the change of magnetic structure of the Ni due to size reduction of nanomagnetic particles. This interpretation will be referred continuously in the following discussion.

Room temperature magnetization–magnetic-field ($m$-$B$) loop for the field applied in the plane of the CM for the same CM as the one employed in the 1 and 2 CNTs is shown in Fig. 2(f). The major hysteresis loops for the Ni in 1 CNTs shown in the figure is narrow and elongated like the typical ones found in granular magnetic systems without explicit saturation, clearly indicating the superparamagnetic behavior of a nanomagnetic particle with diameter below the critical radius. Of course, the shape is not entirely superparamagnetic, since coercivity and remanence are nonzero. Granular solids composed of single domain magnetic properties exhibit superparamagnetic behavior. Although with imperfect superparamagnetism, the magnetic properties of an assembly of noninteracting magnetic particles with a broad distribution of sizes and shapes and randomly distributed easy axes can be described in the framework of the well-known superparamagnetic mode for the Co nanodots formed in this work. While CM in 1 showed a hysteretic loop showing small saturation magnetization, the $M$-$H$ loop for 2 presents large loops showing well defined saturation behavior of a typical ferromagnetic material.[18]

In order to examine effect of the catalytic metal on the field electron emission properties of CNTs, we investigated the field emission current of the CNTs. Figure 3(a) shows the

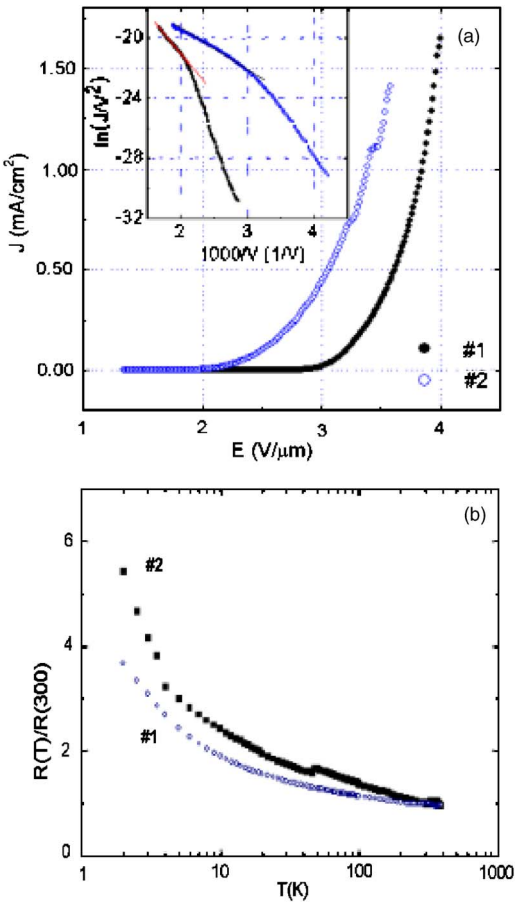


FIG. 3. (Color online) (a) Field emission current vs applied electric field characteristics after initial burn-in. Inset figures show the Fowler-Nordheim plots of the current–electric-field data as shown (a). The linear fit indicates that the electron emission was dominated by the FN tunneling process. (b) Electrical resistivity vs temperature for the CNTs.

dependences of both the emission current and turn-on field of CNTs on the catalytic material. As confirmed through EPR spectra, the stronger ferromagnetic behavior of CNTs, i.e., catalytic metal, resulted in lower turn-on field, suggesting that the electron emission was strongly suppressed or modified due to the catalytic metals that were found at the end of the CNTs. Two main approaches can be used to enhance the field emission: (1) increase the field enhancement factor $\beta$ [estimated from the slope of Fowler-Nordheim (FN) plot], which enhances the effective local field at the emission site, and (2) reduce the work function. In our case, catalyst of 1 existed at the bottom while CM of 2 remained at the top and/or within the inner space of an individual tube. The slow slope of the FN plot in linear region of 2 corresponds to the higher enhancement factor. However, we cannot rule out the possibility of the change in the work function ($\Phi$) due to close contact of Ni residue to CNTs. In our work, for all these samples, higher resistivity as well as larger temperature coefficient of resistivity for 2 CNTs [Fig. 3(b)] corresponded well to the failure of electron emission behaviors in the high field regime, as shown in Fig. 3(a), suggesting that an additional effect of the ferromagnetic metal existed on the tip ends of CNTs besides that of the CNT itself. Especially, the observations of current fluctuation and final catalytic failure at the high field region for 2 are in agreement with the results of previous works, in which the Fe nanotips act as an atomic scale beam splitter suggesting a strong magnetic interaction at the atomic scale apex of the nanosized Fe electron emitter.[15]

In this study, we observed the following. (i) The magnetic nanodots that existed within CNTs grown on $SiO_2$-coated Si substrate for electronic-spin devices showed different magnetic behavior depending on the growth process. (ii) Electron emission threshold for the CNTs with ferromagnetic residuals depended strongly on the magnetic properties of catalyst residuals, although the CNTs had the same ferromagnetic nanodots as impurities, regardless of the thickness of the CM.

Although our observations cannot provide the complete understanding of the catalytic metal effect on the transport behavior, the presence of ferromagnetism of catalysts after the growth of CNTs was clearly confirmed by nondestructive EPR study and their distinct effect on both the electrical and magnetic behaviors and moreover on the field emission behavior of CNTs was revealed. Since confirmed magnetic effect in as-grown vertical CNTs was deduced from our experiment, magnetically modified CNTs could be used as probe in a study of the ferromagnetic proximity effect and spin-dependent transport in a CNT system.

The authors acknowledge the technical helps from KBSI (Seoul Branch), Y. Lee at KIST, J. H. Lee at NDPL, and old colleagues at KIST. This work was supported by Nano Basic Technology of KOSEF and partially by Pure basic Research Group Project (PBRG, 2005) of KRF in Korea. The publication fee of this letter was supported by National Research Laboratory (NRL) Program of KOSEF.

[1] W. A. Dheer, A. Chatelain, and D. Ugarte, Science **270**, 1179 (1995).
[2] P. G. Collines and A. Zettl, Appl. Phys. Lett. **69**, 1969 (1996).
[3] L. Nilsson, O. Groening, C. Emmenegger, O. Kuettel, E. Schaller, L. Schlapbach, H. Kind, J.-M. Bonard, and K. Kern, Appl. Phys. Lett. **76**, 2071 (2000).
[4] Eric Minoux, O. Groening, K. B. K. Teo, H. Dalal, L. Gangloff, J. Ph. Schnell, L. Hudanski, I. Y. Y. Bu, P. Vincent, P. Legagneux, G. A. J. Amaratunga, and W. I. Milnes, Nano Lett. **5**, 2135 (2005).
[5] Yun-Hi Lee, Yoon-Taek Jang, Dong-Ho Kim, Jin-Ho Ahn, and Byeong-Kwon Ju, Adv. Mater. (Weinheim, Ger.) **13**, 479 (2001).
[6] C. C. Chuang, J. H. Huang, C. C. Lee, and Y. Y. Chang, J. Vac. Sci. Technol. B **23**, 772 (2005).
[7] M. Chhowalla, C. Ducati, N. L. Rupesinghe, K. B. K. Teo, and G. A. J. Amaratunga, Appl. Phys. Lett. **79**, 2079 (2001).
[8] K. B. K. Teo, M. Chhowalla, G. A. J. Amaratunga, W. I. Milne, G. Pirio, P. Legagneux, F. Wyczisk, D. Pribat, and D. G. Hasko, Appl. Phys. Lett. **80**, 2011 (2002).
[9] Y. Tu, Z. P. Huang, D. Z. Wang, J. G. Wen, and Z. F. Ren, Appl. Phys. Lett. **80**, 4018 (2002).
[10] S. H. Jo, Y. Tu, Z. P. Huang, D. L. Carnahan, D. Z. Wang, and Z. F. Ren, Appl. Phys. Lett. **82**, 3520 (2003).
[11] A. N. Andriotis, M. Menon, G. Froudakis, and J. E. Lowther, Chem. Phys. Lett. **301**, 503 (1999).
[12] A. N. Andriotis and M. Menon, Phys. Rev. B **60**, 4521 (1999).
[13] Y. Chen, D. T. Shaw, and L. Guo, Appl. Phys. Lett. **76**, 2469 (2000).
[14] H. Murakami, M. Hirakawa, C. Tanaka, and H. Yamakawa, Appl. Phys. Lett. **76**, 1776 (2000).
[15] V. T. Binch, N. Gracia, and S. T. Purcell, *Advances in Imaging and Electron Physics* (Academic, San Diego, 1996), Vol. 12, p. 1–5.
[16] K. Shen, D. L. Tierney, and T. Pietraß, Phys. Rev. B **68**, 165418 (2003).
[17] Yun-Hi Lee, Hoon Kim, Dong-Ho Kim, and Byeong-Kwon Ju, J. Electrochem. Soc. **147**, 3564 (2000).
[18] R. C. Handley, *Modern Magnetic Materials* (Wiley, New York, 2000), Vol. 12, Chap. 12, p. 436.